Photoluminescence in pyridine-based polymers: Role of aggregates

J. W. Blatchford and S. W. Jessen
Department of Physics, The Ohio State University, Columbus, Ohio 43210

L.-B. Lin and T. L. Gustafson
Department of Chemistry, The Ohio State University, Columbus, Ohio 43210

D.-K. Fu, H.-L. Wang, T. M. Swager, and A. G. MacDiarmid
Department of Chemistry, University of Pennsylvania, Philadelphia, Pennsylvania 19104

A. J. Epstein
Department of Physics and Department of Chemistry, The Ohio State University, Columbus, Ohio 43210
(Received 31 May 1996)

We present a study of the morphology dependence of the photoluminescence (PL) properties of the pyridine-based polymers poly(*p*-pyridyl vinylene), poly(*p*-pyridine), and poly(*p*-pyridyl vinylene *p*-phenylene vinylene) (PPyVPV). The photoluminescence of solution samples is characterized by high quantum efficiency (>70% in PPyVPV), weak coupling to vibrational modes (Huang-Rhys parameter ~0.5) and a single-exponential decay (radiative lifetime ~1 ns). On the other hand, film samples display strongly redshifted, featureless emission with low quantum yield (<20%) and highly nonexponential decay dynamics. Through consideration of absorption and excitation spectra, the ''site-selectivity'' of the PL, and the concentration dependence of the PL spectrum, we demonstrate that the redshifted film spectra are a result of the formation of low-energy aggregate sites due to strong interchain interactions. Time-resolved measurements suggest a longer radiative lifetime for the aggregate vs solution, leading to the lower efficiency. Aggregate formation is found to be morphology dependent, and is minimal in ''powder'' samples which are precipitated after polymerization. [S0163-1829(96)06237-6]

I. INTRODUCTION

The role of interchain interactions in the photoluminescence (PL) properties of conjugated polymers is currently a topic of great interest, as well as controversy.[1–5] An important impetus for understanding these properties is the fact that the maximum attainable efficiency of conjugated polymer light emitting diodes[6] is determined in part by the PL efficiency. With few exceptions,[7] it is generally agreed that interchain interactions lead to reduced PL efficiency in these systems. Therefore, a complete understanding of the nature of interchain interactions in conjugated polymers, their role in determining PL efficiency, and means of avoiding the detrimental effects of these interactions is of scientific and technological importance.

A reasonably complete understanding of photophysical processes in conjugated polymers has evolved in recent years, although the details are still under debate. Rauscher and co-workers[8,9] have suggested, based on morphological considerations, that poly(*p*-phenylene vinylene) (PPV) films should be viewed as a collection of oligomers of various length, leading to an inhomogeneously broadened density of states for the system. Photoexcitation produces a *singlet exciton* of mixed Frenkel- and Wannier-like character that is localized to a conjugated segment. The exciton migrates to the lowest-energy (i.e., longest) segments of the sample, leading to redshifted emission. Evidence for such a model comes from measurements of ''site-selective fluorescence,'' wherein the shape and position of the luminescence spectrum is monitored as a function of excitation energy. The work of Rauscher and co-workers demonstrates that while the apparent Stokes shift (redshift) between absorption and emission maxima is large in real samples due to inhomogeneous broadening, the *intrinsic* Stokes shift (i.e., that of ideal, well-extended PPV chains) is quite small, $<100\ \mathrm{cm}^{-1}$. This small value is inconsistent with early electron-phonon based models, which predict a much larger Stokes shift due to geometric relaxation.[10]

While most authors agree that the intrinsic photophysics of luminescent polymers is excitonic, the role of interchain interactions is a topic of widespread debate. The role of the *excimer* (short for ''excited dimer'') recently has been suggested by Jenekhe and Osaheni[3,7] for rigid-rod polymers such as poly(*p*-phenylene-2,6-benzobisoxazole). The excimer is an emissive excited-state complex which is delocalized over two molecular units.[11] The ground state of the excimer is dissociative; that is, the ground state of the dimer spontaneously dissociates into two ground-state molecules. Furthermore, the excimer cannot be directly excited optically. Photoexcitation in excimer-forming systems therefore leads to production of an intramolecular singlet exciton that later delocalizes over two molecules, forming the excimer. Excimer formation is accompanied by a strong geometric distortion along the intermolecular axis that, when combined with the dissociative nature of the ground state, leads to featureless, strongly Stokes-shifted emission in comparison to dilute solution.[11] A classical example of an excimer-forming

system is pyrene in solution.[11] As the solution concentration is increased, the structured pyrene emission is gradually replaced by a featureless excimer band. The absorption spectrum, however, is found to be concentration independent.

A closely related concept is that of the ''polaron pair.'' [1,2,12–14] These entities are suggested to consist of an electron and hole residing on opposite chains bound by their mutual Coulomb attraction. (In comparison, excimers may contain contributions from neutral excited states in addition to charge-transfer states). Yan *et al.* have suggested that the majority of species created on photoexcitation of PPV are polaron pairs. They further suggest that these species are nonemissive, leading to reduced PL quantum efficiency in PPV films. Based on their picosecond photoinduced absorption results, they further suggest that the polaron pair is created only from ''hot'' excitons and not from relaxed ones. Therefore, unlike in the case of the excimer, the branching ratio between emissive intrachain singlet excitons and interchain polaron pairs is determined on a femtosecond time scale.

While excimers exist only in the excited state, interchain interaction may also lead to ground-state interactions, a manifestation of which is the formation of *aggregate states*.[15] These species have been suggested to occur in ''ladder'' polyphenylenes based on photoluminescence[4] and photocurrent[16] measurements. Upon aggregation, both the ground- and excited-state wave functions are delocalized over several polymer chains. The aggregate is therefore directly accessible spectroscopically. The delocalization leads to a redshift in both emission and absorption vs solution. Unlike the excimer, which tends to form spontaneously, the aggregate usually results from a forced proximity of two or more molecules, an example of which is the anthracene sandwich dimer.[15] While the energy of the molecular ground state is lowered upon aggregate formation, the first excited state splits into several distinct levels. The allowedness of transitions to these levels is determined by the alignment of the individual dipoles of the molecules which form the aggregate. Parallel alignment typically leads to a less-allowed or forbidden lowest transition.[15,37] Aggregation therefore leads to reduced PL efficiency in this case.

In this paper, we examine the role of interchain interactions in the fluorescence properties of pyridine-based polymers such as those shown in Fig. 1. These polymers are promising for light-emitting diode applications[17,18] due to their increased oxygen stability over that of PPV and their high electron affinity. In recent publications,[19–21] we have suggested the role of aggregates in the emission of film samples of the pyridine-based polymers. In the present work, we present an extensive study of the luminescence properties of this class of polymers, emphasizing the morphology dependence of spectroscopic properties and of aggregate formation. In Sec. II, the experimental methods are summarized. In Sec. III, we present the results of cw and time-resolved PL studies, as well as measurements of PL quantum efficiencies, absorption spectra, and structural properties of these polymers in various morphologies. In particular, film samples show strongly redshifted luminescence with low quantum yield, which we demonstrate to result from the formation of aggregates. As-precipitated powder samples, on the other hand, behave like solution samples, indicating that

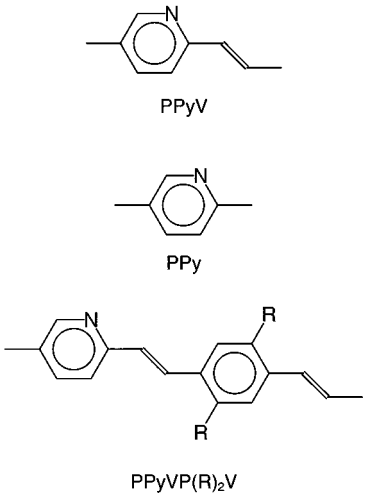

FIG. 1. Repeat units for pyridine-based polymers studied. For the PPyVPV polymer, $R=C_{12}H_{25}$, $OC_{16}H_{33}$ or $COOC_{12}H_{25}$.

aggregate formation is strongly morphology dependent and can be avoided. As such, the powder samples provide a convenient laboratory for the examination of solid-state effects in the absence of aggregate formation. We demonstrate the generality of these phenomena in the pyridine-based systems despite the differing properties of the repeat units. Section IV presents a summary and conclusion for our studies.

II. EXPERIMENTAL

The synthesis routes to each of the pyridine-based polymers studied are reported elsewhere.[22–24] All polymers are precipitated from solution during or after polymerization. This as-precipitated solid we label as ''powder'' in this paper. The powder samples are mixed with KBr and pressed into pellets for study. Some of the powder sample is dissolved to form solution samples of varying concentration. The poly(*p*-pyridyl vinylene) (PPyV) and poly(*p*-pyridine) (PPy) samples are generally soluble in weak acids such as formic acid (HCOOH). The poly(*p*-pyridyl vinylene *p*-phenylene vinylene) (PPyVPV) copolymers are soluble in common organics by virtue of their hydrocarbon sidegroups. In the present work, results are shown for symmetrically substituted copolymers with sidegroups $R=C_{12}H_{25}$, $OC_{16}H_{33}$, and $COOC_{12}H_{25}$. All the solution measurements presented herein for the copolymers were performed in spectroscopic-grade tetrahydrofuran (THF). Film samples were prepared by drop- or spin-casting concentrated solution onto quartz substrates.

The direct absorption measurements were performed on a Perkin-Elmer Lambda-19 UV/VIS/NIR spectrometer. The PL measurements utilized a SPEX Fluorolog or PTI QuantaMaster fluorometer. Solution PL quantum efficiencies were measured on the QuantaMaster fluorometer with respect to a Rhodamine 6G standard and were corrected using accepted values for the refractive indices of the various solvents used. External quantum efficiencies of film samples were measured with the sample placed at one port of an integrating sphere. A low-pass filter was used to block the 440 nm exciting radiation. The excitation beam was chopped at 200 Hz and the PL detected with a Si photodiode and a lock-in amplifier. The measurements were corrected for sample reflec-

tivity and absorption, as well as the leakage of stray excitation light through the filter. Internal quantum efficiencies were calculated from the external efficiencies by multiplying by $2n^2$, where n is the refractive index of the film at the emission wavelength. All refractive indices were estimated to be ~1.9 based on Kramers-Kronig analysis of the reflection spectrum.

X-ray-diffraction (XRD) measurements were performed using a SCINTAG spectrometer in the Bragg scattering geometry. The x-ray wavelength was 0.154 nm, corresponding to the Cu $K\alpha$ line. Samples were mounted on an off-axis Si substrate with silica gel.

The time-resolved PL measurements utilized excitation with ~5 ps pulses centered at 440 nm from a Coherent 700-series synchronously pumped dye laser. These measurements were performed using the time-correlated single-photon counting technique, yielding ~50 ps resolution. All PL decays were collected to 10^4 counts in the peak channel. The incident power was kept low (typically <100 μW) to avoid sample degradation. To examine the time evolution of the PL spectrum, PL decays were taken at ~5 nm intervals and normalized by the collection time, as well as corrected for the spectral response of the monochrometer and detector. The evolution of the total (energy-independent) PL was examined by numerically integrating the single-wavelength decays over energy by applying the trapezoidal rule.

Spectroscopic measurements on solutions were performed in quartz cuvettes. Some of the solutions were bubbled with Ar gas for 5 min prior to measurement; however, this step did not affect the outcome of the experiments and was generally not taken. Measurements on powder and film samples were generally performed in an evacuated cryostat, although the samples were found to be insensitive to air exposure during the time frame of the experiments. Spectroscopic properties of solid samples were checked before and after prolonged exposure to the excitation beam to rule out the effects of photochemical degradation. All measurements were performed at room temperature.

III. RESULTS AND DISCUSSION

A. Fluorescence properties of solutions

Typical absorption (solid), PL (dotted), and PL excitation (PLE, dashed) spectra for representative pyridine-based polymers in dilute solution ($<10^{-5}$ M) are shown in Fig. 2. Weak vibronic structure is observed in the PL spectra; however, no vibronic structure can be distinguished in the absorption spectra. Such diffuse spectra are characteristic of ''floppy'' systems which possess a ring-rotational degree of freedom, due to the generally weak steric hindrance towards ring rotations in these systems.[25–27] At room temperature, a distribution of ground states with differing ring-torsion angles is present, leading to the featureless absorption spectrum. The excited state of these systems is generally more planar due to aromatic-to-quinoid conversion,[26,28,29] leading to the Stokes-shifted PL spectrum.

Unlike in the case of PPV,[30] for all the pyridine-based polymers studied the PLE spectrum closely follows the absorption spectrum, in accord with Vavilov's law.[11] Such a result indicates that internal conversion (phonon emission) to the first excited state is more efficient than other processes,

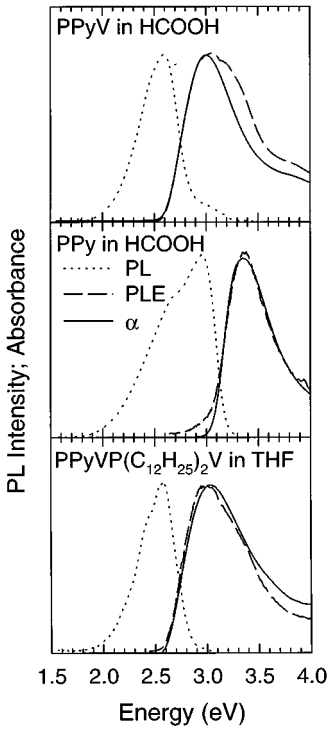

FIG. 2. Absorption (solid), photoluminescence (PL, dotted) and PL excitation (PLE, dashed) spectra for dilute solutions ($<10^{-5}$ M) of PPyV in HCOOH (upper), PPy in HCOOH (middle), and PPyVPV in THF (lower).

such as radiative decay, in dissipating energy in the polymer. In MEH-PPV, a discrepancy between the PLE and absorption spectra of dilute solutions has been suggested to originate from a subpicosecond internal conversion to the ground state which becomes more likely under high-energy excitation.[30] For the pyridine-based polymers, such a process apparently does not occur efficiently.

Figure 3 shows the PL spectrum (solid) of $OC_{16}H_{33}$-derivatized PPyVPV in dilute solution. Unlike the spectra of Fig. 2, the PL spectrum of this copolymer shows more pronounced vibronic structure due to hydrogen bonding between the OC_{16} sidegroups and the vinylene bridge,[25,27] which assists the planarity of the molecule in the ground and excited states. Assuming strong coupling to a single vibrational mode of wave number ν_0, the relative in-

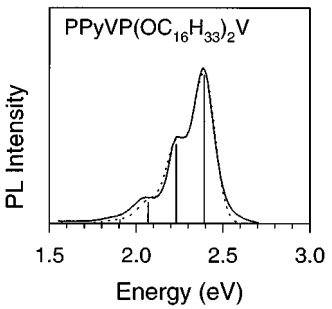

FIG. 3. PL of 10^{-5} M $PPyVP(OC_{16}H_{33})_2V$ in THF (solid line). Dotted line is fit to Huang-Rhys expression, Eq. (1) (see text).

TABLE I. PL quantum efficiencies, observed PL lifetimes, and calculated radiative lifetimes for pyridine-based polymers in dilute ($<10^{-5}$ M) solution.

Polymer	PL quantum efficiency	Observed lifetime	Radiative lifetime
PPyV	0.22	439 ps	2.00 ns
PPy	0.10	170 ps	1.89 ns
PPyVP($C_{12}H_{25}$)$_2$V	0.76	715 ps	941 ps
PPyVP($OC_{16}H_{33}$)$_2$V	0.80	660 ps	825 ps
PPyVP($COOC_{12}H_{25}$)$_2$V	0.90	629 ps	698 ps

tensities $I(n)$ of the various vibronics n in the PL spectrum can be described by the Huang-Rhys parameter, S, given by[31]

$$I(n)=\frac{e^{-S}S^n}{n!}. \quad (1)$$

The parameter S is proportional to the change in elastic energy upon geometric relaxation. The dotted line in Fig. 3 represents a fit to Eq. (1) above (assuming a Gaussian broadening), and the vertical lines in the figure represent the various vibronics. The fit corresponds to a Huang-Rhys parameter of $S=0.53$. For comparison, $S=0.47$ has been suggested for gel-aligned MEH-PPV.[32] For PPyVPV, the strongly coupled vibration is found to be at $\nu_0=1302$ cm^{-1}. A similar mode (1300 cm^{-1}) provides the vibronic structure in the PL spectrum of distyryl benzene (the three-ring oligomer of PPV), where it has been assigned to the vinylne C═C stretch.[27] The parameter S is related to the geometrical relaxation energy, $E_{\rm rel}$, via the relation $S=E_{\rm rel}/hc\nu_0$. For PPyVPV, we find $E_{\rm rel}=86$ meV, indicating relatively weak geometrical relaxation for the singlet exciton.[31]

Table I shows the PL efficiencies and lifetimes for the pyridine-based polymers in dilute solution. The efficiencies are generally quite high, especially for the PPyVPV copolymers. The PPy efficiency is low, possibly due to the age and quality of the sample. All PL decays were found to be nearly (>90%) single-exponential. The PL decays were generally independent of wavelength, although the PPy sample shows a slight redshift to the PL with time.[33] The single-exponential decay together with the close agreement between PLE and absorption spectra allows the computation of the radiative lifetime $\tau_{\rm rad}$ from the quantum efficiency (QE) and the observed PL lifetime $\tau_{\rm obs}$: $\tau_{\rm rad}=\tau_{\rm obs}/{\rm QE}$.[11] These results are also shown in Table I. The radiative lifetime is found to be ~1–2 ns for all polymers studied, similar to results reported for substituted PPV in solution.[34]

The concentration dependence of the PL spectrum (upper) and decay (lower) is demonstrated in Fig. 4 for PPyVPV. The PL spectrum is nearly independent of concentration, with the slight difference due to self-absorption at higher emission energies. This concentration independence suggests that the pyridine-based polymers do not have a strong tendency towards excimer formation. In contrast, in excimer-forming systems like pyrene,[11] redshifted excimer-like emission usurps the single-molecule emission at relatively low concentrations ($<10^{-3}$ M). The PL decay at 2.6 eV of the concentrated PPyVPV solution closely mirrors the single-exponential behavior of dilute solution. The PL decay at 2.0 eV of the concentrated solution, however, shows a slight deviation from single-exponential behavior that becomes most evident after ~2 ns. As will be discussed below, we believe this additional long-lived component to be due to interchain association which is a precursor of aggregation in film samples. Similarly, in PPyV solutions, the emission and its time dynamics are concentration independent in the 10^{-6}–10^{-1} M range.

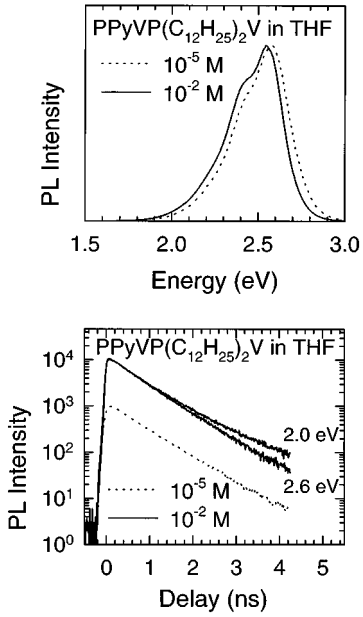

FIG. 4. PL spectrum (upper) and PL decays (lower) of 10^{-5} M (dotted lines) and 10^{-2} M (solid lines) PPyVP($C_{12}H_{25}$)$_2$V in THF. For the concentrated solution, PL decays are shown for 2.0 and 2.6 eV emission. Dilute solution PL decay is for 2.6 eV emission.

B. Fluorescence of solid samples: aggregate formation

While the PL of solution samples shows the high quantum efficiency characteristic of aromatic molecular systems, the PL of film samples does not share this property. This is demonstrated in Table II, which shows the measured external and calculated internal PL quantum efficiencies of the film samples. These values were measured under 440 nm excitation and were corrected using the PLE spectrum. They therefore represent the maximum PL efficiency of the sample. In contrast to the solution results, the internal quantum efficien-

TABLE II. Measured external and calculated internal quantum efficiencies for pyridine-based polymers. Internal quantum efficiencies were calculated assuming a refractive index of 1.9.

Polymer	Ext. QE	Int. QE
PPyV	0.015	0.11
PPy	0.010	0.07
PPyVP($C_{12}H_{25}$)$_2$V	0.040	0.29
PPyVP($OC_{16}H_{33}$)$_2$V	0.003	0.02
PPyVP($COOC_{12}H_{25}$)$_2$V	0.025	0.18

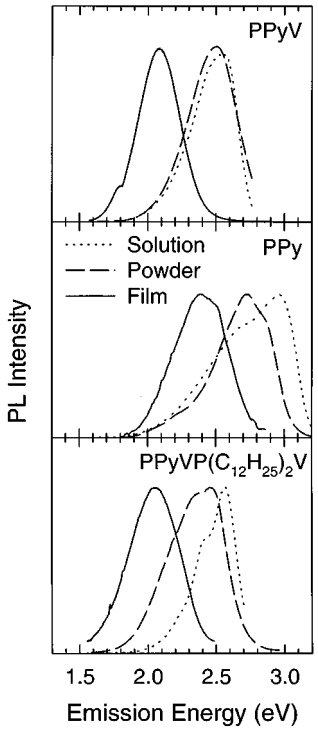

FIG. 5. PL spectrum of solution (dotted), powder (dashed) and film (solid) samples of PPyV (upper), PPy (middle), and PPyVPV (lower).

cies of the films are all quite low, typically 1/2 to 1/3 of the solution value. The internal quantum efficiency of the $PPyVP(OC_{16}H_{33})_2V$ film is particularly low, only about 0.02. Infrared-absorption studies indicate that the origin of the extremely low efficiency in this particular copolymer is the formation of C═O sites due to oxygen exposure.[35] These sites act as efficient luminescence quenchers.[36] The susceptibility of the OC_{16} copolymer to oxygen attack is likely the result of the electron-donating character of the sidegroups. Significant C═O formation is not present in the other copolymers or in PPyV and PPy.

The origin of the reduced quantum efficiency of films becomes apparent when the cw spectroscopic properties of the film samples are compared with those of the solution. The PL spectrum of film (solid line) samples is compared with that of solution (dotted) and powder (dashed) for representative pyridine-based polymers in Fig. 5. (Again, the powder samples are distinguished from the film samples by the fact that powder samples are precipitated from solution during polymerization.) In all cases, the film spectrum is redshifted by ~0.5 eV vs solution and is featureless. In contrast, the powder spectrum more closely resembles the solution result in all cases, particularly in the case of PPyV (upper portion of the figure). Below, we demonstrate that the redshifted film spectra result from the formation of aggregate states in these samples. The fact that the film and powder spectra are different indicates that aggregate formation is *morphology dependent*. In addition to the difference between films and powders, films cast from different solvents generally display different PL spectra, again indicating a morphology dependence to the emission. Finally, films cast from *the same solvent* also have been seen to have different PL spectra depending on the preparation conditions. In particular, spin-cast films, for which the solvent evaporates rapidly, generally show less of a redshift than drop-cast films, for which the solvent evaporates slowly.

Several intrinsic and extrinsic mechanisms that might produce a redshifted film spectrum can be ruled out. First, a redshifted spectrum vs solution may simply result from the fact that the index of refraction of the film sample is different from that of the solution.[37] This and related ''solid-state'' phenomena are ruled out by the fact that the film and powder spectra are different, despite similar refractive indices. Furthermore, the effects of self-absorption can be ruled out, as the film and powder samples have similar optical densities in all cases. Oxygen contamination of film samples can also be ruled out as the source of the redshift from infrared-absorption studies.[35] Indeed, the film samples were found to be extremely resistant to photooxidation (with the exception of the OC_{16} copolymer). Furthermore, attempts to deliberately photo-oxidize the powder samples did not lead to a redshifted PL spectrum for these samples. Finally, deep traps due to residual solvent can be ruled out. The solvents used for the casting of the PPyVPV films (THF, chloroform) are quite volatile and are therefore not expected to remain in the film samples. Attempts to remove residual solvent by a combination of high vacuum and heating did not result in a reduced redshift for the film spectrum.

Although we have eliminated a number of factors which might produce a redshift in film samples, a distinction between aggregate formation and excimer formation cannot be made based on PL data alone. The concentration independence of the solution data presented above are already suggestive of aggregate formation rather than excimer formation, as excimers are expected to form spontaneously in solution; whereas aggregates usually result from ''forced'' interaction due to packing considerations. To fully rule out excimer formation, however, one must examine other spectroscopic properties. In particular, if excimer formation were responsible for the redshifted emission of films, one would expect the absorption and PLE spectra of film samples to be identical to those of solution. Furthermore, the Stokes shift of the emission should be large in the case of the excimer. On the other hand, since aggregates can be directly accessed optically, one expects redshifted absorption and PLE spectra and a relatively small Stokes shift for the emission in the aggregate case.

The direct absorption spectra of solutions (dotted), powders (dashed) and films (solid lines) are shown in Fig. 6 for the same polymers as in the previous figure. The film absorption spectra are redshifted from the solution result by a similar amount as in the case of the PL (~0.5 eV), showing additional low-energy oscillator strength below the solution absorption onset. While these spectra are not corrected for reflection, the reflectivity of the samples was measured and actually peaks well below the solution absorption edge. Therefore, a reflection correction would actually *enhance* the absorption spectrum below 2.5 eV in all cases. Additional complications arise from scattering losses, which likely contribute substantially to the tail of the absorption below 2.2 eV in the PPyV and PPyVPV spectra. Nevertheless, in the PPy spectrum, where such losses are minimal, it is clear that the film spectrum is substantially redshifted from the solution

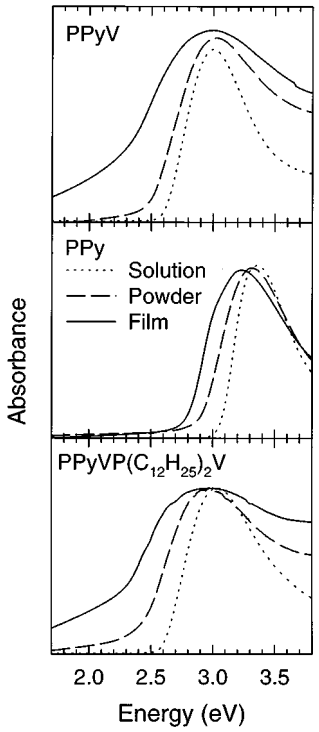

FIG. 6. Absorption spectrum of solution (dotted), powder (dashed) and film (solid) samples of PPyV (upper), PPy (middle), and PPyVPV (lower).

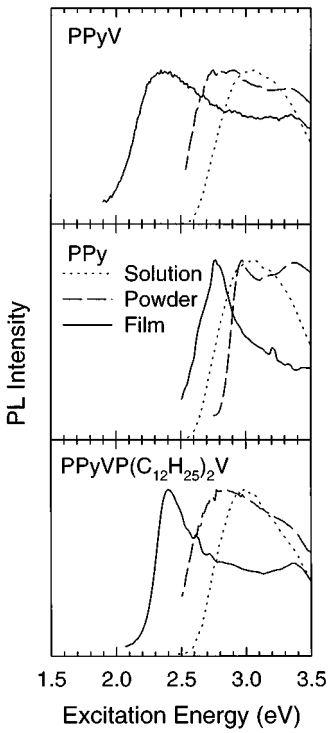

FIG. 7. PLE spectrum of solution (dotted), powder (dashed) and film (solid) samples of PPyV (upper), PPy (middle), and PPyVPV (lower).

result, indicating the presence of additional, low-energy, directly accessible excitations in film samples. This result is in direct contrast with the expectations for excimer formation, as in general excimers cannot be directly excited.[15]

As with the PL spectra, the powder absorption spectra closely follow the solution spectra, particularly in the case of PPyV. The PPy and PPyVPV powder absorption spectra deviate somewhat from the solution result, as with the PL spectra. Again, these results point to the morphology dependence of aggregate formation in these polymers.

Figure 7 shows the PLE spectra for solutions, powders and films of the various polymers. Here, the powder PLE spectra are somewhat different from the corresponding solution spectra. This deviation reflects the fact the powder samples are optically thick, whereas the solution samples are optically thin. Unlike the absorption spectrum, which is essentially the logarithm of the quantum efficiency for absorption, the PLE directly measures the quantum efficiency for emission (i.e., no logarithm involved), resulting in a ''flattening'' of the spectrum at high optical densities. The film PLE spectra are dramatically different from the solution spectra, peaking in a region where the solution PLE and absorption are essentially zero. The peak of the film PLE is close to the peak of the PL spectrum in all cases, suggesting a small intrinsic Stokes shift. Again, the redshifted PLE spectra of film samples suggests additional, low-energy, directly accessible states in film samples, inconsistent with excimer formation.

While the PLE spectra suggest a small Stokes shift for the emitting species, this value can be directly measured using the site-selective fluorescence technique, as was discussed in the Introduction. Ideally, one should use a tunable laser to measure such effects, as the spectral purity of such a source allows monitoring of emission wavelengths that are very close to the exciting line. An upper bound on the intrinsic Stokes shift can be obtained, however, by using a conventional PL spectrometer, which allows measurement of emission to within 5 nm of the exciting line. The PL spectra at varying excitation energies are shown for films of the pyridine-based polymers in Fig. 8. For the various spectra, the exciting wavelength is indicated by the downward arrow. In all cases, substantial luminescence can be excited with low-energy radiation. Furthermore, the peak of the emission under low-energy excitation is different from that under high-energy excitation, indicating site-selective effects (i.e., multiple emitting sites in the sample). An upper bound on the intrinsic Stokes shift can be estimated from the difference between the excitation energy and the peak of the resulting emission under low-energy excitation. For PPyV, the emission under 2.04 eV excitation is peaked at 1.98 eV, indicating that the intrinsic Stokes shift of the low-energy emission is a very small 60 meV. This is again in contrast with expectation for excimer emission, for which the Stokes shift should be quite large ($\sim$0.5 eV).

An additional argument for the formation of aggregates comes from near-field scanning optical microscopy (NSOM), a technique which allows direct spatial imaging of emission and absorption in polymer films to a resolution of 100 nm.[38–40] Recent NSOM measurements of PPyV films indicate that emission is localized in partially aligned regions of the film of domain size $\sim$200 nm.[21] While this size is too large to correspond to a single aggregate, it does suggest that aggregates are most likely to form in aligned regions of the sample, as expected.

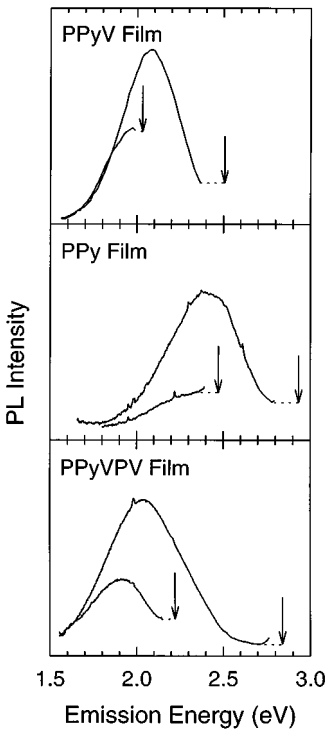

FIG. 8. PL spectra of film samples of PPyV (upper), PPy (middle), and PPyVPV (lower), demonstrating site-selective effects. Arrows indicate excitation energy for each spectrum.

C. Time-resolved luminescence

We now consider the time evolution of the PL spectrum in light of the cw results. As was mentioned above, the solution PL decays are nearly single-exponential with a radiative lifetime of 1–2 ns, and the decays are independent of wavelength. In contrast, the film PL decays are highly nonexponential and show a strong wavelength dependence. Figure 9 displays the time evolution of the PL spectrum of a PPyVPV film. For reference, the cw film and solution PL

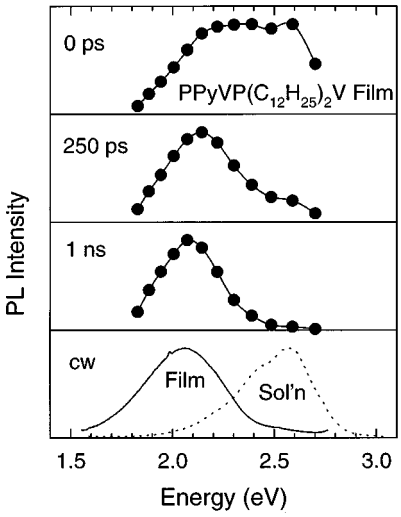

FIG. 9. PL spectrum of PPyVPV film at 0 ps, 250 ps, and 1 ns delay following excitation at 2.8 eV. Lower frame shows cw PL spectra of PPyVPV solution (dotted) and film (solid) samples.

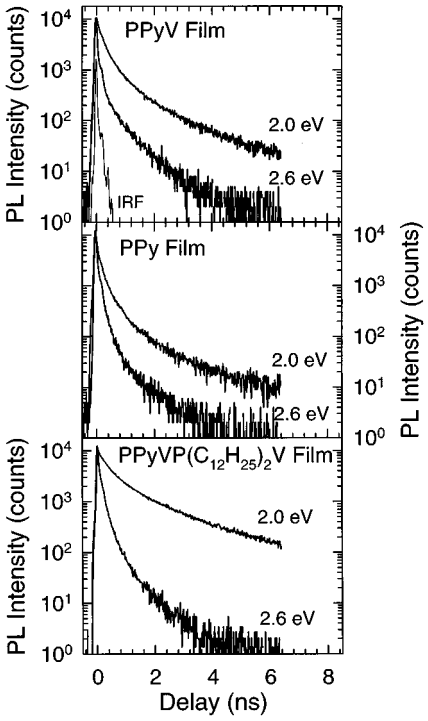

FIG. 10. PL decays of PPyV (upper), PPy (middle), and PPyVPV (lower) films excited at 2.8 eV. Decays are shown for 2.0 and 2.6 eV emission, as indicated. Instrument response (IRF) is shown in the upper portion of the figure.

spectra are shown in the lower frame. In comparison with the cw spectra, the 0 ps spectrum displays both solutionlike (2.6 eV) and aggregatelike (2.0 eV) components in roughly equal proportions. By 250 ps, the solutionlike component is greatly diminished and by 1 ns has vanished. The aggregatelike component decays with little or no spectral diffusion.

A complimentary picture, the evolution of the PL at fixed wavelength vs time delay, is shown for three representative polymers in Fig. 10. In all cases, the decays are highly nonexponential at all wavelengths. The 2.6 eV solutionlike decay is initially very fast, at the resolution of the experiment. (The instrument response is denoted IRF in the upper portion of the figure.) This fast decay suggests rapid diffusion of excitons to aggregate sites. The diffusion is likely facilitated by efficient Förster transfer due to the strong overlap between the intrachain solutionlike emission and the aggregate absorption.[15] On the other hand, the 2.0 eV aggregatelike emission is very long lived. The PPyVPV decay at this energy has a time constant of about 2.5 ns, greater than the predicted radiative lifetime of the solution emission (941 ps). Similar long-lived decays are seen for PPyV and PPy films, as seen in the figure. The very long-lived observed lifetime for the aggregate emission, together with the low quantum yield of the film PL, suggests that the radiative lifetime of the aggregate is much longer than that of the single-chain emission. The ~30% quantum yield of the PPyVPV film emission places a lower bound of about 8 ns on the aggregate radiative lifetime. From the Einstein relations,[11] a longer radiative lifetime is associated with a less allowed transition. A less-allowed optical transition is expected for aggregates in which the individual transition dipoles are aligned parallel to

each other, as in a card-pack arrangement.[15,37] As the longer radiative lifetime indicates a lower probability for radiative decay, provided nonradiative decay pathways are similar for the aggregate and interchain emission, *a long radiative lifetime implies reduced quantum efficiency for the aggregate.*

Despite the presence of aggregates in the film samples, the film absorption spectrum is actually quite similar to that of the solution (e.g., the absorption maxima are at nearly the same energy), indicating that 2.8 eV excitation creates mainly intrachain excitons in the films which later migrate to the aggregate sites. Nevertheless, a rise to the aggregate emission could not be detected in any of the samples studied. The observation of such a rise is hindered by the very rapid initial migration to aggregate sites, which is likely faster than the experimental resolution, as well as the spectral overlap between the solutionlike and aggregate emission spectra. Substantial sub-50-ps migration to aggregate sites is evidenced by the ''0 ps'' spectrum of the PPyVPV film, which suggests that at least half of the initial ($<$50 ps) emission is from the aggregates. Since emission from aggregate excitons apparently occurs with lower quantum yield than the intrachain emission, it can be concluded that the initial *density* of excited aggregates (i.e., the number of aggregates excited within the 50 ps resolution) is actually greater than the density of intrachain species. It is therefore not surprising that a rise to the aggregate emission could not be detected.

While the time-resolved data of the film samples is clearly consistent with energy transfer from intrachain excitons to aggregate sites, it could be argued that such behavior is an artifact of exciton migration in an inhomogeneously broadened density of states. In this scenario, excitons migrate to longer chains where the emission energy is lower but the radiative lifetime is essentially unchanged. It is important to rule out this possibility by considering the behavior of the *total* PL; i.e., by integrating out the energy dependence of the PL to get the net change in the total exciton population. The result is shown for the representative polymers in Fig. 11, where the total emission from the film samples (solid line) is compared with that of the solution. In comparison to the single-exponential solution decay, the total film PL is again highly nonexponential, showing a rapid initial decay followed by a long-lived component. The retention of these features of the single-wavelength decays of Fig. 10 indicates that these decay components are not simply an artifact of inhomogeneous broadening, but are due to the presence of multiple emission components (intrachain and aggregate).

The time evolution of the PL spectrum of powder samples is considered in Fig. 12. Here we only consider PPyV powders, which, from the cw PL data of Fig. 5, are the least affected by aggregate formation. The single-wavelength decays of the powder samples retain much ($\sim$90%) of their single-exponential character of the solution; however, a spectral redshift is seen with time, again suggestive of exciton migration. We note that the spectral diffusion in the powder samples is much less than that of the film samples: at 2 ns, the 2.0 eV powder emission is roughly two times the emission at 2.6 eV, assuming both decays are normalized at $t=0$. In contrast, for film samples, at 2 ns the 2.0 eV emission is over one order of magnitude greater than the 2.6 eV emission. Furthermore, unlike in the case of the film samples, for the powder samples the total (energy-integrated)

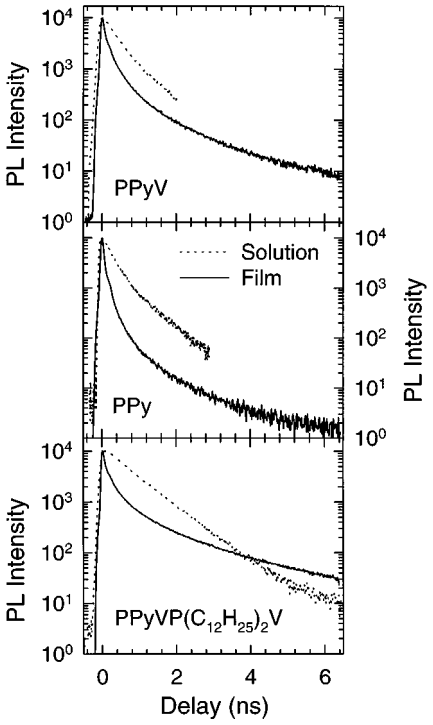

FIG. 11. Energy-integrated PL decays for PPyV (upper), PPy (middle), and PPyVPV (lower) films (solid lines) excited at 2.8 eV. Solution decays (at PL maximum) are shown for comparison (dotted lines).

PL decay closely follows that of the solution, as is shown in the lower portion of Fig. 12. The small discrepancy between the solution and powder total PL decays is likely due to enhanced triplet production in the powder samples.[41] These

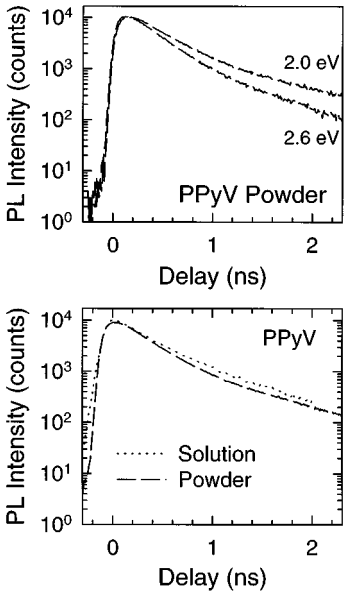

FIG. 12. PL decays at 2.0 and 2.6 eV (upper) and energy-integrated PL decay (lower) for PPyV powder (dashed lines) excited at 2.8 eV. Solution PL decay (2.6 eV) is shown for comparison (dotted line) in the lower portion of the figure.

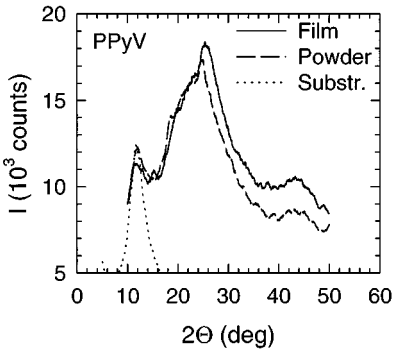

FIG. 13. X-ray-diffraction spectrum of PPyV powder (dashed) and film (solid). Dotted line represents background due to off-axis Si substrate. X-ray wavelength is 0.154 nm (Cu $K\alpha$).

results suggest that the spectral diffusion observed in powder samples is an artifact of exciton migration in an inhomogeneously broadened density of states,[42] and *not* due to the presence of multiple emission components, as would result from aggregation. Therefore, the time-resolved data are consistent with the observation that substantial aggregation does not occur in PPyV powder samples.

D. Morphology

Although the PPyV powder and film samples show large differences in their photophysical properties, their morphological properties are actually quite similar. Figure 13 shows the XRD spectrum of PPyV powder (dashed line) and film (solid line), together with the contribution from the Si substrate (dotted line). Both the powder and film samples lack substantial structural order. On the other hand, the NSOM measurements[21] discussed briefly above indicate large regions ($\sim$200 nm) of gross alignment for the PPyV film samples. We therefore suggest that the formation of aggregates in the pyridine-based polymers is more closely related to liquid-crystalline order than crystalline order.

PPyVPV samples have been shown to exhibit a sanidic (boardlike) liquid-crystalline phase at elevated temperatures.[24] Preliminary measurements indicate that PPyVPV is also liquid crystalline in solution in a variety of solvents.[43] We therefore suggest the following origin for the morphology dependence of aggregate formation in this system: powder samples are precipitated from a solvent in which the polymer is very poorly soluble, leading to a disordered, coil-like morphology. On the other hand, film samples are prepared from solvents in which the polymer dissolves well, leading to liquid-crystalline order in concentrated solutions. As the solvent evaporates upon film formation, the correlations between neighboring chains persist, leading to grossly aligned regions in the film. Aggregate sites are likely to form in these regions. The sanidic liquid-crystalline order in solution is suggestive of a card-pack arrangement for the aggregate alluded to above, leading to a less-allowed lowest optical transition.

In PPyVPV, liquid crystalline order is likely facilitated by the hydrocarbon sidegroups, which may crystalize in films and concentrated solutions. Nevertheless, the formation of aggregates is not exclusively due to sidegroup crystallization, as PPyVPV polymers with noncrystallizing sidegroups also show aggregate formation.[44] Furthermore PPyV and PPy do not possess any such sidegroups. Nevertheless, a similar concept may explain the presence of aggregates in the film samples of PPyV and PPy: films are cast from a ''good'' solvent leading to better interchain registry than in powders, which precipitate from a ''bad'' solvent. While PPy is known to be rigid-rod-like in solution,[23] thereby facilitating aggregation upon film formation, little is known about the conformation of PPyV in solution. Light-scattering studies of concentrated solutions will be helpful in cementing these ideas.

IV. SUMMARY AND CONCLUSIONS

In summary, cw spectroscopic results point to the existence of low-energy sites in film samples, resulting in redshifted emission vs solution. The absence of these sites in solution indicates that they originate from interchain interaction. The fact that these sites can be directly accessed optically rules out excimer formation as their origin and strongly argues for the formation of aggregate sites in the film samples. The formation of aggregates is apparently detrimental to PL efficiencies, as is evidenced by the reduced efficiencies of film samples vs solution. Time-resolved measurements indicate rapid (sub-50-ps) diffusion of intrachain excitons to aggregate sites following photoexcitation. The long lifetime observed for the aggregate emission implies a less-allowed lowest optical transition for the aggregate, leading to the reduced PL efficiency. While x-ray studies show that film samples lack crystalline order, NSOM measurements demonstrate the existence of large partially aligned regions in film samples where the aggregates are likely to form. We suggest that the formation of these aligned regions is facilitated by the solvent from which the film is cast.

Powder samples generally behave like solution samples, indicating that aggregate formation is morphology dependent. The powders are precipitated from poor solvents, thereby explaining the lack of aggregate formation in these samples in light of the discussion above. The results for powder samples demonstrate that aggregate formation may be avoided in these systems by careful control of disorder.

ACKNOWLEDGMENT

This work was supported in part by the Office of Naval Research.

[1] M. Yan, L. J. Rothberg, F. Papadimitrakopoulos, M. E. Galvin, and T. M. Miller, Phys. Rev. Lett. **73**, 744 (1994).

[2] M. Yan, L. J. Rothberg, E. W. Kwock, and T. M. Miller, Phys. Rev. Lett. **75**, 1992 (1995).

[3] S. A. Jenekhe and J. A. Osaheni, Science **265**, 739 (1994).

[4] U. Lemmer, S. Heun, R. F. Mahrt, U. Scherf, M. Hopmeier, U. Siegner, E. O. Gobel, K. Mullen, and H. Bassler, Chem. Phys. Lett. **240**, 373 (1995).

[5] I. D. W. Samuel, G. Rumbles, and C. J. Collison, Phys. Rev. B **52**, R11 573 (1995).

[6] J. H. Burroughes, D. D. C. Bradley, A. R. Brown, R. N. Marks, K. Mackay, R. H. Friend, P. L. Burns, and A. B. Holmes, Nature (London) **347**, 539 (1990).
[7] J. A. Osaheni and S. A. Jenekhe, Macromol. **27**, 739 (1994).
[8] U. Rauscher, L. Schutz, A. Greiner, and H. Bassler, J. Phys. Condens. Matter **1**, 9751 (1989).
[9] U. Rauscher, H. Bassler, D. D. C. Bradley, and M. Hennecke, Phys. Rev. B **42**, 9830 (1990).
[10] F. X. Bronold, A. Saxena, and A. R. Bishop, Phys. Rev. B **48**, 13 162 (1993).
[11] J. B. Birks, *Photophysics of Aromatic Molecules* (Wiley Interscience, London, 1970).
[12] E. L. Frankevich, A. A. Lymarev, I. Sokolik, F. E. Karasz, S. Blumstengel, R. H. Baughmann, and H. H. Hörhold, Phys. Rev. B **46**, 9320 (1992).
[13] J. W. P. Hsu, M. Yan, T. M. Jedju, L. J. Rothberg, and B. R. Hseih, Phys. Rev. B **49**, 712 (1994).
[14] H. A. Mizes and E. M. Conwell, Phys. Rev. B **50**, 11 243 (1994).
[15] M. Pope and C. E. Swenberg, *Electronic Processes in Organic Crystals* (Oxford University Press, New York, 1982).
[16] A. Köhler, J. Grüner, R. H. Friend, K. Müllen, and U. Scherf, Chem. Phys. Lett. **243**, 456 (1995).
[17] D. D. Gebler, Y. Z. Wang, J. W. Blatchford, S. W. Jessen, L. B. Lin, T. L. Gustafson, H. L. Wang, T. M. Swager, A. G. MacDiarmid, and A. J. Epstein, J. Appl. Phys. **78**, 4264 (1995).
[18] Y. Z. Wang, D. D. Gebler, L. B. Lin, J. W. Blatchford, S. W. Jessen, H. L. Wang, and A. J. Epstein, Appl. Phys. Lett. **68**, 894 (1996).
[19] J. W. Blatchford, S. W. Jessen, L. B. Lin, T. L. Gustafson, A. J. Epstein, D. K. Fu, H. L. Wang, T. M Swager, and A. G. MacDiarmid, in *Electrical, Optical and Magnetic Properties of Organic Solid State Materials III*, edited by L. R. Dalton, A. K. Y. Jen, G. E. Wnek, M. F. Rubner, C. Y. C. Lee, and L. Y. Chiang, MRS Symposia Proceedings No. 413 (Materials Research Society, Pittsburgh, 1996), p. 671.
[20] A. J. Epstein, J. W. Blatchford, Y. Z. Wang, D. D. Gebler, S. W. Jessen, L. B. Lin, T. L. Gustafson, D. K. Fu, H. L. Wang, T. M. Swager, and A. G. MacDiarmid, Synth. Met. **78**, 253 (1996).
[21] J. W. Blatchford, T. L. Gustafson, A. J. Epstein, D. A. Vanden Bout, J. Kerimo, D. Higgins, P. F. Barbara, D. K. Fu, T. M. Swager, and A. G. MacDiarmid, Phys. Rev. B (to be published).
[22] M. J. Marsella, D.-K. Fu, and T. M. Swager, Adv. Mater. Res. **7**, 145 (1995).
[23] T. Yamamoto, T. Maruyama, Z. Zhou, T. Ito, T. Fukuda, Y. Yoneda, F. Begum, T. Ikeda, S. Sasaki, H. Takezoe, A. Fukuda, and K. Kubota, J. Am. Chem. Soc. **116**, 4832 (1994).
[24] D. K. Fu, M. J. Marsella, and T. M. Swager, Polym. Prepr. Am. Chem. Soc. Div. Polym. **36**, 585 (1995).
[25] O. Lhost and J. L. Bredas, J. Chem. Phys. **96**, 5279 (1992).
[26] F. Momicchioli, M. C. Bruni, and I. Baraldi, J. Phys. Chem. **76**, 3983 (1972).
[27] T. E. Bush and G. W. Scott, J. Phys. Chem. **85**, 144 (1981).
[28] J. L. Brédas, R. R. Chance, and R. Silbey, Phys. Rev. B **26**, 5843 (1982).
[29] J. W. Blatchford, T. L. Gustafson, and A. J. Epstein (unpublished).
[30] L. J. Rothberg, M. Yan, F. Papadimitrakopoulos, M. E. Galvin, E. W. Kwock, and T. M. Miller, Synth. Met. (to be published).
[31] G. F. Imbusch, in *Luminescence Spectroscopy*, edited by M. D. Lumb (Academic, London, 1978), p. 1.
[32] T. W. Hagler, K. Pakbaz, K. F. Voss, and A. J. Heeger, Phys. Rev. B **44**, 8652 (1991).
[33] L. B. Lin, Ph.D. thesis, The Ohio State University, 1995.
[34] L. Smilowitz, A. Hays, A. J. Heeger, G. Wang, and J. E. Bowers, J. Chem. Phys. **98**, 6504 (1993).
[35] S. W. Jessen, Ph.D. thesis, The Ohio State University, 1996.
[36] M. Yan, L. J. Rothberg, F. Papadimitrakopoulos, M. E. Galvin, and T. M. Miller, Phys. Rev. Lett. **73**, 744 (1994).
[37] R. S. Becker, *Theory and Interpretation of Fluorescence and Phosphorescence* (Wiley Interscience, New York, 1969).
[38] E. Betzig, J. K. Trautman, T. D. Harris, J. S. Weiner, and R. L. Kostelak, Science **251**, 1468 (1991).
[39] E. Betzig and J. K. Trautman, Science **257**, 189 (1992).
[40] D. A. Higgins and P. F. Barbara, J. Phys. Chem. **99**, 3 (1995).
[41] J. W. Blatchford, S. W. Jessen, L. B. Lin, J. J. Lih, T. L. Gustafson, A. J. Epstein, D. K. Fu, M. J. Marsella, T. M. Swager, A. G. MacDiarmid, S. Yamaguchi, and H. Hamaguchi, Phys. Rev. Lett. **76**, 1513 (1996).
[42] B. Mollay, U. Lemmer, R. Kersting, R. F. Mahrt, H. Kurz, H. F. Kaufmann, and H. Bassler, Phys. Rev. B **50**, 10 769 (1994).
[43] D. K. Fu (private communication).
[44] J. W. Blatchford and A. J. Epstein (unpublished).